

Ultra-high Performance Fiber Reinforced Concrete Panel Subjected to Severe Blast Loading

Viet-Chinh Mai^{@*}, Ngoc-Quang Vu[#], Van-Tu Nguyen[#], and Hoang Pham[#]

[@]Department of Civil Engineering, Kumoh National Institute of Technology, Gumi, South Korea

[#]Institute of Techniques for Special Engineering, Le Quy Don Technical University, Ha Noi, Viet Nam

*E-mail: maivietchinh@lqdtu.edu.vn

ABSTRACT

Experimental studies play a crucial role in shedding light on the dynamic behaviour of structures under blast loading. However, high costs and complicated technical requirements, particularly for full-scale structures, are still huge disadvantages to conduct such a series of tests. Hence, the finite element method is much needed to provide supplementary information to previous experiments and to enable further parametric studies without testing. This article presents a numerical investigation carried out to understand the behaviour of ultra high performance fiber reinforced concrete (UHPFRC) panels under severe blast loading. The authors designed a subroutine with eight numbers of solution-dependent state variables, 32 mechanical constants, integrated with the Abaqus program to analyze the dynamic behaviour of UHPFRC against multiple blast impacts, using the Johnson-Holmquist 2 damage model incorporating both the damage and residual strength of the material. The subroutine was validated by comparing the simulation results with test results. For the purpose of estimating the structural response of the UHPFRC panel subjected to blast loading, other studying scenarios were considered by varying input parameters, including the thickness of the panel, stand-off distance, and steel reinforcement bar volume. The variations in deflection, strain, and damage of the UHPFRC panel, as well as the steel reinforcement strain, were also evaluated. Through important obtained results, the UHPFRC panel is strongly recommended for a protective barrier installed in the vicinity of critical infrastructure against severe blast loading

Keywords: Ultra high performance fiber reinforced concrete; UHPFRC; Blast loading; Panel; Numerical model; Johnson-Holmquist 2 damage model

1. INTRODUCTION

Nowadays due to an increase in the explosive incidents attributable to industrial accidents and terrorist attacks, it becomes necessary to study the response of structures subjected to blast loading. Protecting civilian buildings or military infrastructure from the threat of any explosive activities is one of the most important challenges for structural engineers. In particular, for strategically important complexes such as government buildings, a higher level of blast resistance is required due to the increased risk of uncontrolled explosions. Conventional concrete is a principal material used widely for civilian constructions and military structures. However, this material is characterized by the brittle property, which prone to be damaged under tensile stress and cracks¹. To improve the dynamic performance and overcome such defects of normal concrete against special loading conditions, advanced concrete materials with different additions have been developed. UHPFRC defined as high strength, ductile material formulated by combining cement, silica fume, quartz silica sand, crushed quartz, super-plasticizer, and fibres with compressive strength exceeding values of 150N/mm² and more^{2,3}. In UHPFRC, the water to binder ratio is lower than 0.25, high content of binder,

which leads to the absence of capillary porosity and adding fibres in the mix to ensure a ductile behaviour. Due to these characteristics, UHPFRC possesses superior properties such as advanced strength, higher durability, and long-term stability than normal concrete⁴⁻⁷.

There were many experiments of normal concrete or high strength concrete under blast load⁸⁻¹⁶. However, due to the high technical requirements, high costs of manufacturing UHPFRC, tests on UHPFRC members under blast load are very limited. Burrell¹⁷ took the experiment of a total of 13 half-scaled steel fibre reinforced concrete columns under blast load. They found out that the important role of fibre in reducing the number of secondary blast fragments. Furthermore, maximum and residual deflection in UHPFRC columns remarkably decreases compared to normal concrete. Ellis¹², *et al.* conducted an experimental program on UHPFRC panels to validate a multi-scale model. Base on the results, they concluded that packing, volume fractions, and fibre geometry are all factors that significantly influence the resistance of UHPFRC panels under blast loading. Juechun¹⁸, *et al.* researched the behaviour of UHPFRC columns subjected to blast load. In their study, many field tests were conducted to investigate the behaviour of UHPFRC columns under blast load. Compared to the high strength concrete, UHPFRC columns not only showed higher resistance under the over pressures and shock waves resulted

from explosive but also decreased the maximum displacements. Rizwanullah and Sharma studied the role of critical parameters of UHPFRC structures under blast load. They concluded that compared to high strength concrete and normal concrete, UHPFRC increased capacity to disseminate a large amount of energy during blast loading and reduce the severe damage in the structure after blast load¹⁹. Mao²⁰, *et al.* used the Concrete Damage Model in LS-DYNA to evaluate the behaviour of UHPFRC panels under blast loads, which took into account the strain rate effect. Cavill²¹, *et al.* took experimental studies on seven UHPFRC panels. These panels were tested with varying stand-off distances, including 30m, 40m, and 50m. Overall, obtained results proved the positive response of UHPFRC panels under blast loading, showing high ductility and no sign of severe damage. Moreover, by evaluating peak deflection compared to span, the remarkable energy absorb of the UHPFRC panel was demonstrated. The obtained results are significant, yet due to the security restrictions requirement, the exact designs of the UHPFRC panel was not revealed.

In order to obtain more accurate predictions of the dynamic behaviour of UHPFRC structures in general and UHPFRC panels in particular under blast load, a numerical simulation method is needed. Using numerical models result in reducing the large numbers of costly experiments. This study demonstrates the potential of using UHPFRC material for protecting important structures subjected to blast load. In this paper, the implementation of numerical models to investigate the response of UHPFRC panels under severe explosions was carried out. Modelling the UHPFRC panel under blast load using a computer-aided program is significant in providing supplementary knowledge for blast loading resistance design. The numerical simulation was conducted using the ABAQUS software combined with a subroutine, which is designed by the authors. This method is based on the explicit numerical model for problems associated with large deformation and multi-loading environments. The results were compared to experiments to validate the accuracy of the subroutine. As mentioned above, there are only a few tests of UHPFRC structure in this field, and ABAQUS software has not supported the input parameters for UHPFRC. Therefore, choosing the proper material model and using supported subroutine is crucial to calibrate these input parameters following the structural behaviour of UHPFRC under blast load.

2. MATERIAL MODEL

JH-2 is the second version of the Johnson–Holmquist (JH-1) damage model^{22,23}, which is able to simulate the behaviour of brittle materials such as concrete under blast load including the strain-rate effects, dilatation and pressure-strength dependence caused by damage. Based on the JH-2 model, the yield strength degrades with damage accumulation. The strength is defined in terms of the equivalent stress as follows:

$$\sigma^* = \sigma_i^* - D(\sigma_i^* - \sigma_f^*) \quad (1)$$

where, σ_i^* denotes the normalized intact equivalent stress; D ($0 \leq D \leq 1$) denotes the damage parameter.

The equation of strength can be defined in a general form by normalizing the terms in Eqn (1) to the equivalent stress at

the Hugoniot elastic limit (HEL):

$$\sigma_{HEL} = 3 / 2 (HEL - P_{HEL}) \quad (2)$$

where, P_{HEL} is the pressure at the HEL. Eqn (1) can be rewritten as:

$$\sigma^* = \sigma / \sigma_{HEL} \quad (3)$$

In the JH-2 model, it is assumed that in case of undamaged and fully damaged material state, the equation of the strength can be expressed as a function of the pressure and strain rate:

$$\sigma_i^* = A(P^* + T^*)^N / (1 + C \ln \dot{\epsilon}^*) \leq \sigma_i^{max} \quad (4)$$

$$\sigma_f^* = B(P^*)^M (1 + C \ln \dot{\epsilon}^*) \leq \sigma_f^{max} \quad (5)$$

where, σ_i^{max} ; σ_f^{max} denotes the strength limits;

A; B; C; M, and N are the material parameters.

The normalized pressure is defined as:

$$P^* = P / P_{HEL} \quad (6)$$

where, P is the actual pressure. The normalized maximum tensile hydrostatic pressure can be written as:

$$T^* = T / T_{HEL} \quad (7)$$

where, T is the maximum tensile pressure supported by the material. The strain rate is given by:

$$\dot{\epsilon}^{pl} = \dot{\epsilon} / \dot{\epsilon}_0 \quad (8)$$

where, $\dot{\epsilon}^{pl}$ is the equivalent plastic strain rate. The JH-2 model assumes that the damage increases along with the plastic strain as follows:

$$D = \sum \frac{\Delta \dot{\epsilon}^{pl}}{\dot{\epsilon}_f^{pl}(P)} \quad (9)$$

$$\dot{\epsilon}_f^{pl} = D_1(P^* + T^*)^{D_2} \quad (10)$$

where, $\dot{\epsilon}^{pl}$ is the increment of the equivalent plastic strain and $\dot{\epsilon}_f^{pl}(P)$ is the equivalent plastic strain at failure. D_1 and D_2 are material constants.

The pressure-volume relationship of a material is defined as:

$$P = \begin{cases} K_1\mu + K_2\mu^2 + K_3\mu^3 & (\mu \geq 0 - \text{compression}) \\ K_1\mu & (\mu < 0 - \text{tension}) \end{cases} \quad (11)$$

where, K_1 , K_2 , K_3 are the material constants; $\mu = \rho / \rho_0 - 1$ with ρ ; ρ_0 are the current and reference densities, respectively. When a material fails, an additional pressure increment ΔP is included, following expression:

$$P = K_1\mu + K_2\mu^2 + K_3\mu^3 + \Delta P \quad (12)$$

If the material is damaged, the elastic energy ΔU decreases owing to the decrease in strength. The decrease in elastic energy is converted into the potential energy through an increase in the pressure increment

$$\Delta P: \Delta P_{t+\Delta t} = -K_1\mu_{t+\Delta t} + \sqrt{(K_1\mu_{t+\Delta t} + \Delta P_t)^2 + 2\beta K_1\Delta U} \quad (13)$$

where, $0 \leq \beta \leq 1$ is the fraction of the elastic energy increase converted into potential energy.

3. MODELLING OF UHPFRC PANEL

This study assumes that the UHPFRC panel exposed to a single extreme event from an independent impact is a blast. Researching on the possible secondary effect of temperature dependence and fire after blast loading on structure, which is another complicated and time-consuming issue, has not been performed. It should also be noted that the remarkable characteristic of blast load is high magnitude in a very short period²⁴ For these reasons, the model was only analysed for 0.3 seconds when the panel reached permanent deflection after the explosion. Moreover, for the scenario of an external blast, the heat generated by the explosion can be dispersed quickly into the environment. Clearly, for a very short time of 0.3 seconds, it is possible to ignore the temperature dependence of the UHPFRC panel when analysing the model. In the numerical model, a general-purpose linear brick element C3D8R with reduced integration (1 integration point) was chosen for the UHPFRC panel. C3D8R type element is suitable to model concrete material related to the cracking and damage in tension, crushing of concrete in compression, large strain, and creep. 2 node linear displacement element T3D2 was adopted for steel reinforcement bar assumed to deform by axial stretching only. The embedded technique is used to specify the interaction between steel reinforcement bars and concrete, including embedded region and host region, where the number of degrees of freedom at each node on the embedded region is equal to the host region²⁵. The acceptable mesh size for the numerical model depends on the blast scenario. Luccioni²⁶, *et al.* studied the size effects of structures under the blast, using hydrocodes. They concluded that a 10 cm dimension of mesh is suitable enough for the analysis of wave propagation. A model can be meshed with coarser size to get qualitative results. Nevertheless, due to the limitation of the processor in the computer, it should be considered carefully when analyzing the model with a small mesh size. In this study, a chosen 5cm mesh size is completely suitable for numerical simulation analysis.

Based on the theory of the JH2 damage model, the authors created a subroutine program on the platform of ABAQUS software, which is a general finite element analysis package for modeling the nonlinear mechanics of structures and their interactions. The subroutine with eight numbers of solution-dependent state variables, 32 mechanical constants, integrated with the ABAQUS 2017 program to analyze the dynamic behaviour of UHPFRC against multiple blast impacts. The material parameters for UHPFRC are listed in Table 1. These material parameters are referenced from the studies of the UHPFRC plate under the high-velocity impact of a deformable projectile.

The CONWEP blast loading model was selected in this study. CONWEP (Conventional Weapons Effects) is a specific calculation tool utilizing the equations and curves of TM 5-855-1^{28,29}, was implemented into ABAQUS. The realistic overpressure amplitudes, including both positive and negative phase, is the main advantage of using CONWEP. On the other hand, based on a user-defined amount of TNT at a given distance from the explosion source, other blast wave parameters can be calculated.

Table 1. Material parameters for UHPFRC

Variable	Description	UHPFRC
ρ (Ton/mm ³)	Density	2.55e ⁻⁹
f_c (MPa)	Compressive strength	158
f_t (MPa)	Tensile strength	8.4
G (MPa)	Shear modulus	33200
A	Failure Surface constant	0.79
B	Failure Surface constant	0.79
C	Failure Surface constant	0.007
$\dot{\epsilon}_0$	The reference strain rate	1
S_{max}	Material constant	12.5
D_1/D_2	Material constant	0.05/1
P_{HEL}	The pressure at the HEL	19
K_1 (MPa)	Equation of state constant	8.5
K_2 (MPa)	Equation of state constant	17.1
K_3 (MPa)	Equation of state constant	20.8

4. RESULTS AND DISCUSSION

4.1 Validation of the Proposed Model

In this section, three numerical models of UHPFRC panels subjected to blast loading were calculated. Three panels A, B, C have the same dimensions of 3.5 m x 1.3 m x 0.1 m and the stand-off distance from the detonation point is 9 m, 7 m, and 12 m, respectively. UHPFRC panel dimensions, reinforcement bar ratio, and the stand-off distance of detonation point in simulation models are identical to the tests of Mao. The results were compared to the experiments of Mao²⁰ in terms of deflection and damage state after the explosion to verify the accuracy of the proposed model. In the tests of Mao²⁰, *et al.*, the compressive strength of UHPFRC is 170MPa. However, due to limited experimental data, the authors chose 158MPa compressive strength of UHPFRC for this simulation. The input parameters of UHPFRC with 158MPa compressive strength was verified in the study of Yu²⁷, *et al.* Configuration of UHPFRC panel, TNT charge, and 3D Model in ABAQUS are shown in Fig. 1

Figures 2(a) and 2(b) shows blast wave pressure during time history and energy results from blast simulation. The maximum blast overpressure, P_{so} , for a high explosive charge of 100kg

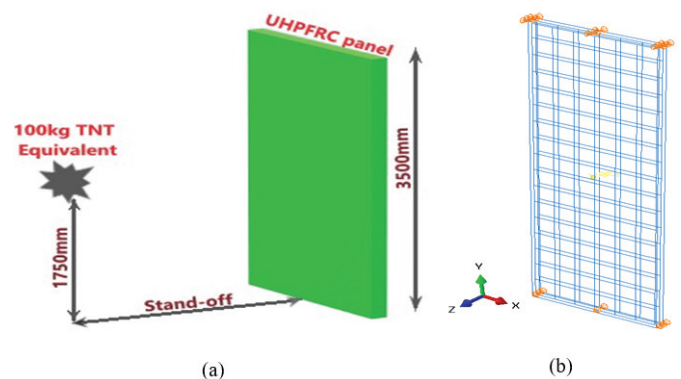


Figure 1. Layout of TNT charge - (a) UHPFRC panel and (b) 3D Model in Abaqus.

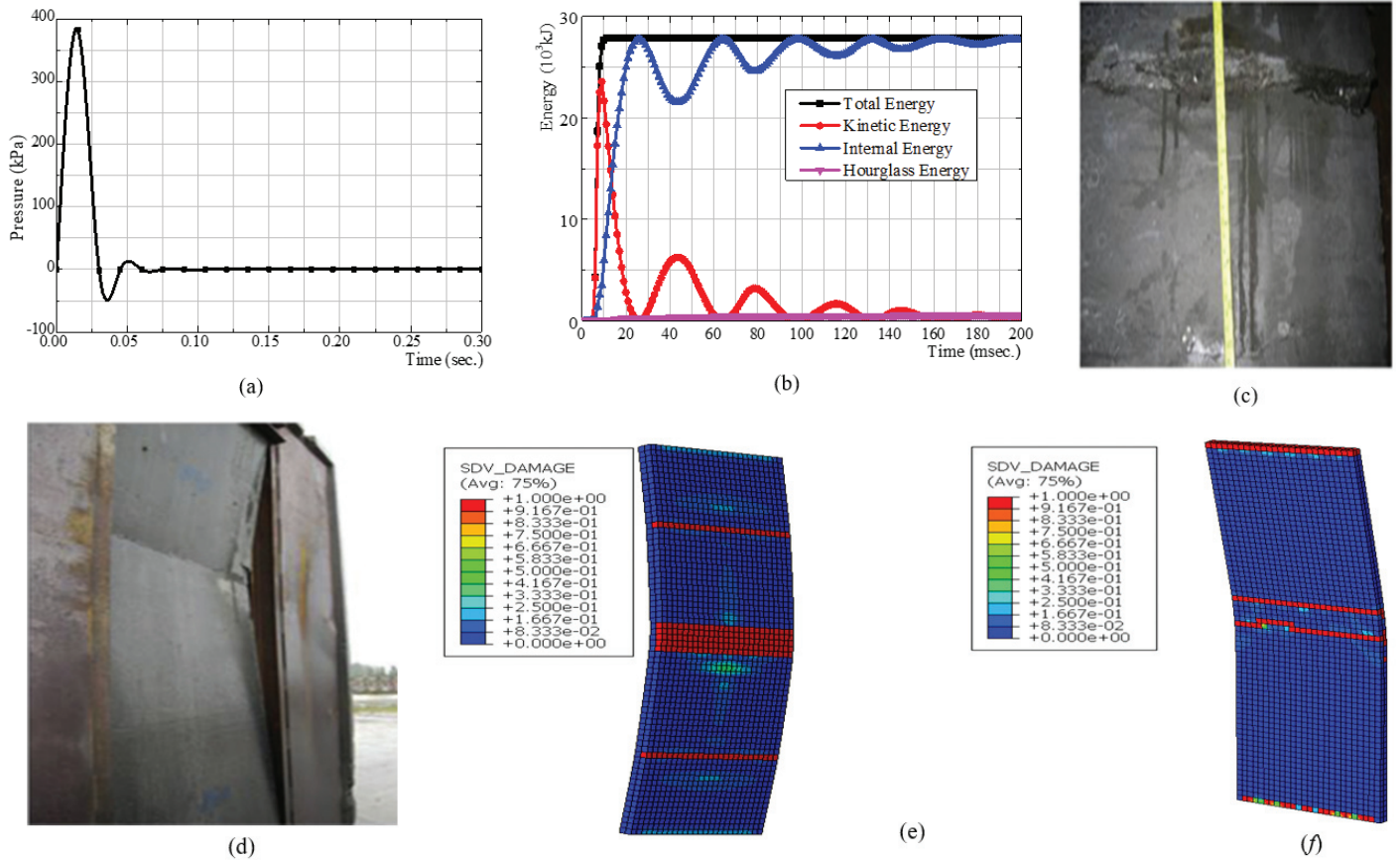


Figure 2. Blast wave pressure- (a) Time history and (b) Energy results from blast simulation, (c) & (d) Damage of Panel C in Lei's test, and (e) & (f) Damage of Panel C in simulation.

TNT equivalent in 9 m stand-off distance, is nearly 400 kPa at the arrival time of 12.5 ms. Hourglass energy shows artificial strain energy (ALLAE for the whole model). The smaller value of hourglass energy indicates more accurate simulation results. For the blast loading calculation model, the hourglass energy must be less than 10 % of the internal energy³⁰. Based on Fig. 2(b), one see that 0.5 kJ of the hourglass energy, which is 1.8% of the largest internal energy (27.7 kJ) and it proves the accurate simulation results of the model.

In Mao's test, horizontal minor cracks were observed on the front and rear faces of panel A. This result is similar to the simulation result with a negligible damage rate and limited cracks. For panel B with the closer of blast loading point distance, more horizontal cracks appeared on the rear face of the panel. For panel C in Mao's test, a severe crack can be observed (Figs. 2(c) and 2(d)). It same as the simulation result in the red region with the damage variable of 1, depicted in Figs. 2(e) and 2(f). The highest damage variable depends on the fracture strength correspond to the value of 1. The maximum deflection from the simulation results is also compared with Mao's tests. The peak deflection of panels is shown in Table 2 and Fig. 3 (Panel A-100m). One can see that the deflection of panels in Mao's test is a little lower than the simulation result.

4.2 Parametric Study

In this section, the UHPFRC panel models under explosive loading are studied by varying the input parameters, including

Table 2. Maximum mid-span deflection of panels

Panel	Deflection (mm)	
	Mao's test	simulation's result
A	110	146.1
B	210	240.2
C	180	210.5

panel thickness, stand-off distance, and steel reinforcement bar volume.

4.2.1 Effect of Thickness Parameter

The dimension of the panel is 3.5m x 1.3m (same to Panel A). It contains a 3.4 % steel reinforcement bar volume and a 9 m stand-off distance from the detonation point. The material parameters for UHPFRC are listed in Table 1. The numerical models were analysed by varying panel thickness: 150 mm, 120 mm, 100 mm, and 80 mm, respectively. Base on the parametric study carried out for panel thickness in Fig. 3(a), it was observed that the maximum mid-span deflection of panel decreased as the thickness of the panel increased for the given blast load scenarios. In particular, a 150 mm panel showed a maximum mid-span deflection of 45.7 mm, which is almost 6 times smaller than 80 mm panel with 262.8 mm of peak deflection. The panel thickness increased twice times and the peak deflection decreased almost 6 times, respectively. Obviously, the thickness affected considerably the panel deflection.

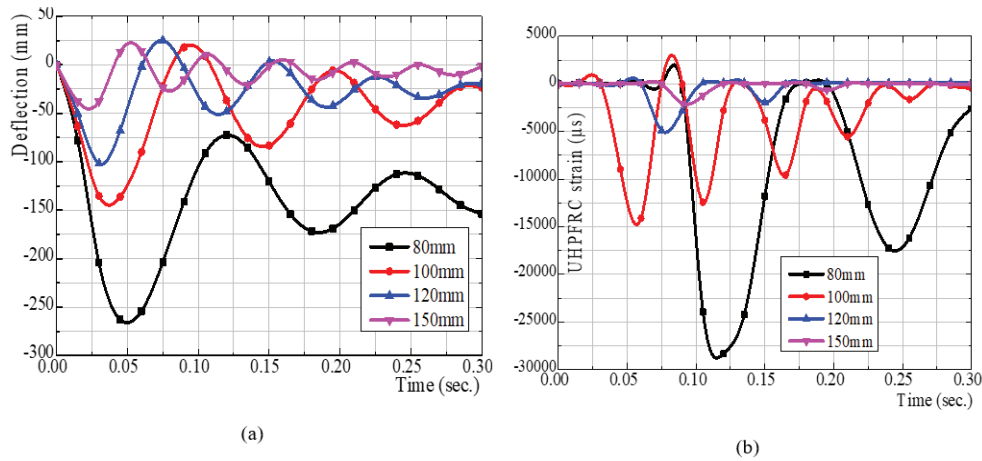


Figure 3. (a) Maximum mid-span deflection of panel and (b) strain of UHPFRC element.

The strain of the UHPFRC panel is shown in Fig. 3(b). Actually, it tends to be similar to the mid-span deformation of the panel, which gradually increased as the panel thickness decreased and reached its maximum value with a thickness of 80 mm. Fig. 4 and Table 3 show the damage of the UHPFRC panels in various thicknesses. It reveals that decreasing the panel thickness leads to the variation on the structural behaviour of the UHPFRC panel. To be more precise, damage mode of flexural failure (concentrated in the mid-span of the panel) was prone to transform into damage mode including flexural failure and shear failure (near the support of panel). UHPFRC panel tends to be failed in the shear mode in the impulsive region and failed in the flexural mode in the quasi-static region. However, although the thickness of the panel reduced significantly, plastic deformation and damage at the edge of the panel expanded slowly. The serious shear failure at the edge of the panel appeared only in the case of 80mm thickness, which is the red region with the damage variable of 1 (see Figs. 4(c) and 4(d)). This result can be explained by high ductility and high strain rate of UHPFRC material under dynamic load.

4.2.2. Effect of Stand-off Distance Parameter

The total energy released by a detonation in the form of a blast wave and the stand-off distance is the crucial parameters in researching structure under blast load. The Hopkinson–Cranz or cube root method is the most widely form of blast

Table 3. Damage state of UHPFRC panel after blast loading (percentage by volume)

Panel thickness (mm)	Light damage	Moderate damage	Severe damage	Collapse
80	17.3%	4.8%	20.2%	-
100	12.1%	1.9%	11.6%	-
120	7.8%	1.2%	8.1%	-
150	4.0%	0.8%	5.7%	-

load scaling, presented in the equation^{31,32}

$$Z = \frac{R}{W^{1/3}} \tag{14}$$

where W is the charge weight, which is defined as the equivalent mass of TNT (100 kg for this research) and R is the stand-off distance from the blast loading. Smith³³, *et al.* researched the scaled distance of Z to identify blast loading conditions for each regime. Base on obtained results, the far-field regime, $3.97 < Z$, defined as the loading cases in which the standoff distance is very high. The near field regime has scaled distance $1.19 < Z < 3.97$ and the close-in regime notion includes the very close distance of blast load, which means $Z < 1.19$. In this section, the dimension of the panel is the same as Panel A (3.5m x 1.3m x 0.1m), including 3.4% of steel reinforcement bar volume, calculated for 4 cases of stand-off distance: 9 m, 7 m, 5 m, and 2 m (see Table 4).

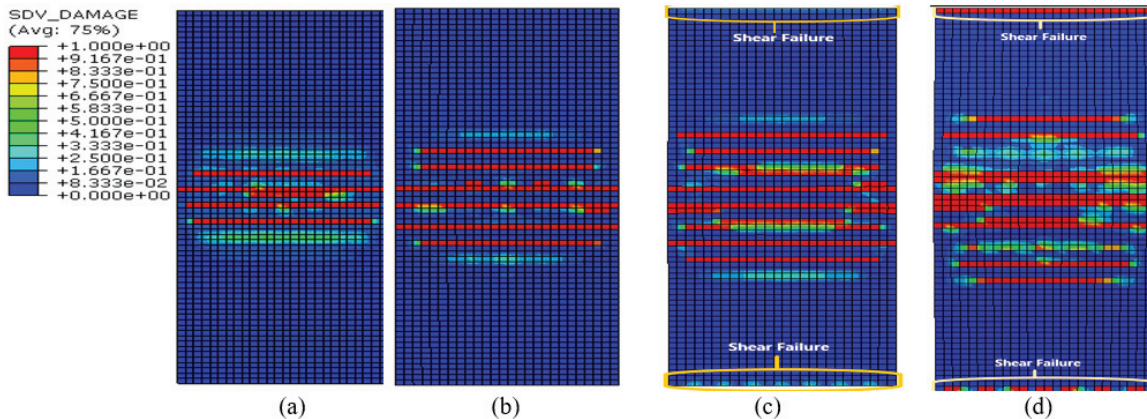


Figure 4. Damage of panel after blast load (a) 150 mm, (b) 120 mm, (c) 100 mm, and (d) 80 mm.

Table 4. Scaled distance for this study

R (m)	Z (m/kg ^{1/3})	Case of study scaled distance
9	1.94	Near field
7	1.5	Near field
5	1.08	Close in
2	0.43	Close in

Based on Fig. 5 and Table 5, careful observation of structural behaviour and damage state reveals that for all considered cases, decreasing the stand-off distance leads to the increment on both the deflection and strain of the UHPFRC panel. Stand-off distance decreased by a half resulted in nearly 4 times increment on peak deflection of the panel, from 146 mm to 554 mm. The severe damage percentage of the panel increased 3 times (11.6% to 34.2%) while the stand-off distance reduced from 9 m to 5 m. Besides, the increment on peak deflection for the close-in regime of blast scenario is much more noticeable than the near field regime. For the near field regime, due to enough stand-off distance, blast wave with duration is the same as the natural period of the panel.

Table 5. Damage state of UHPFRC panel after blast load (percentage by volume)

Stand-off distance (m)	Light damage	Moderate damage	Severe damage	Collapse
9	12.1%	1.9%	11.6%	-
7	18.2%	5.5%	19.7%	-
5	24.7%	9.3%	34.2%	-
2	-	-	-	100%

The structural behaviour of the panel was affected by pressure and impulse. For the close-in regime, the natural period of the panel is higher than the duration of loading and the loading is impulsive. Consequently, the impulsive-control region was formed. Specifically, as this distance decreased to the critical value (2m for this study), the panel was completely collapsed. Impulse caused serious distortion and collapse of the UHPFRC panel.

The damage state of the panel was closely reflected by the strain result in steel rebar and concrete strain (Figs. 5c and 5d). The strain result of the UHPFRC element and steel rebar strain showed a similar trend as the result of deflection. For

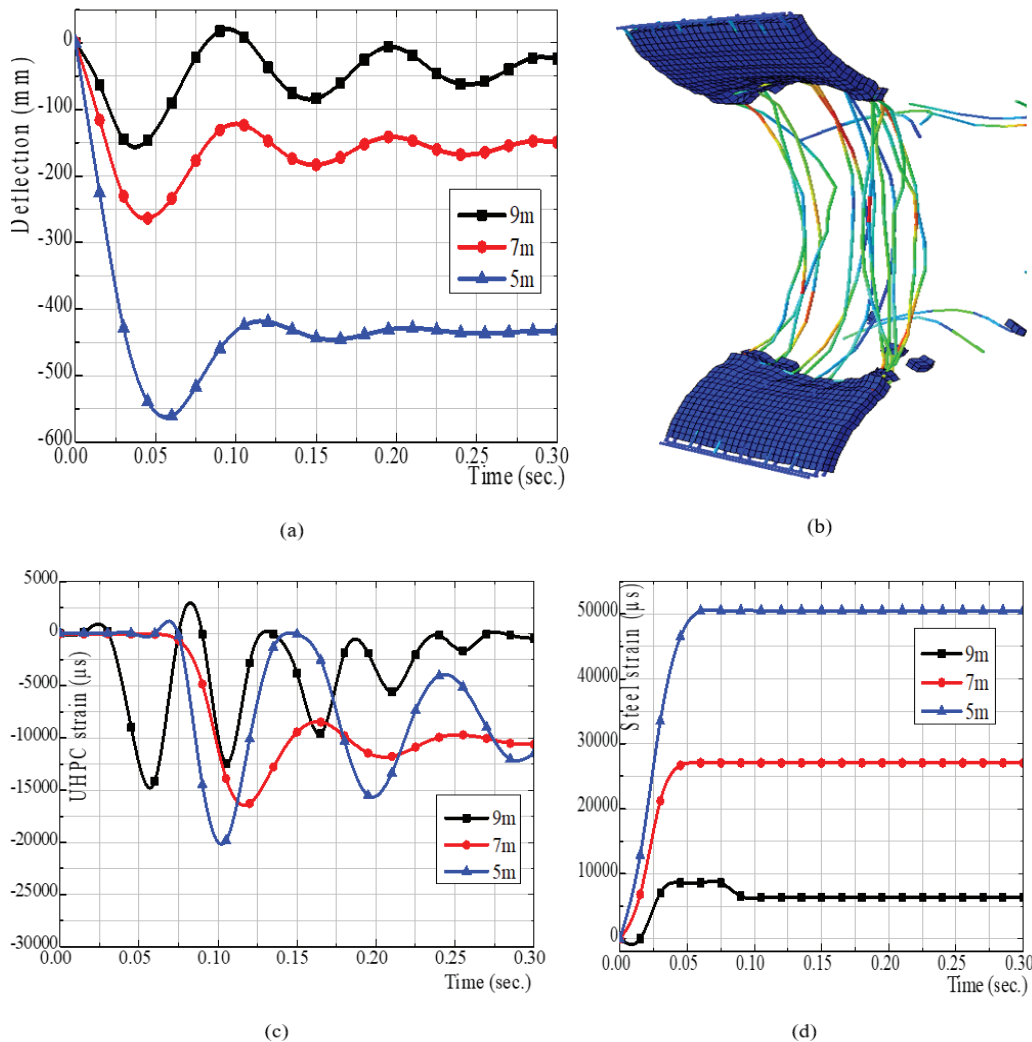


Figure 5. (a) Mid-span deflection, (b) the collapse of the panel in 2m stand-off distance, (c) the strain of UHPFR element, and (d) strain of steel bar.

example, the strain of steel rebar increased more than 5 times as the stand-off distance decreased by 2 times (8597 μ s for 9m stand-off distance and 50505 μ s for 5 m stand-off distance). This indicated that the stand-off distance not only significantly affected the damage state of the panel but also the strain of the panel.

4.2.3. Effect of steel reinforcement ratio parameter

In order to have a better understanding of the dynamic behaviour of the UHPFRC panel under blast load, four numerical models were investigated with various steel reinforcement bar volume, 3.4%, 1.7%, 1%, and 0.3%, respectively. To shed light on the relationship between reinforcement steel ratio and blast loading resistance of UHPFRC panel, two different scenarios with the stand-off distance of 19m and 9m, were also considered. The other input parameters of the panel including dimension and material property are identical to the above section.

Table 6 and Fig. 6 describe the damage state, maximum mid-span deflection and strain of panel after the explosion, from which one can see that in the far-field regime, peak deflection variation is quite small, increasing from 49.9 mm (3.4% of steel reinforcement ratio) to 68.3 mm (0.3% of steel reinforcement ratio). The steel reinforcement bar did not considerably provide

Table 6. Damage state of UHPFRC panel after blast loading (9 m stand-off distance)

Steel reinforcement by volume (%)	Light damage (%)	Moderate damage (%)	Severe damage (%)	Collapse
3.4	12.1	1.9	11.6	-
1.7	17.3	4.3	16.7	-
1	20.6	6.5	21.9	-
0.3	23.9	8.2	27.4	-

more resistance to the panel under blast load. Nevertheless, under the near field regime, the steel reinforcement bar started to provide clear extra resistance to the UHPFRC panel and plays an important role in the UHPFRC panel to resist blast loading. In the near field regime, peak deflection increased almost 2 times, from 146.1 mm (3.4% of steel reinforcement ratio) to 270.1 mm (0.3% of steel reinforcement ratio). The effect of the steel reinforcement ratio on the panel strain shows a similar effect. For instance, in the 9m stand-off distance of the explosion scenario, the strain of steel bar increased 4 times, from 8597.6 μ s to 34311.8 μ s (see Fig. 6(d)). The strain of the UHPFRC element increased 3 times, from 14118 μ s to 41000 μ s (see Fig. 6(c)) while decreasing the steel reinforcement ratio from 3.4 % to 0.3 %.

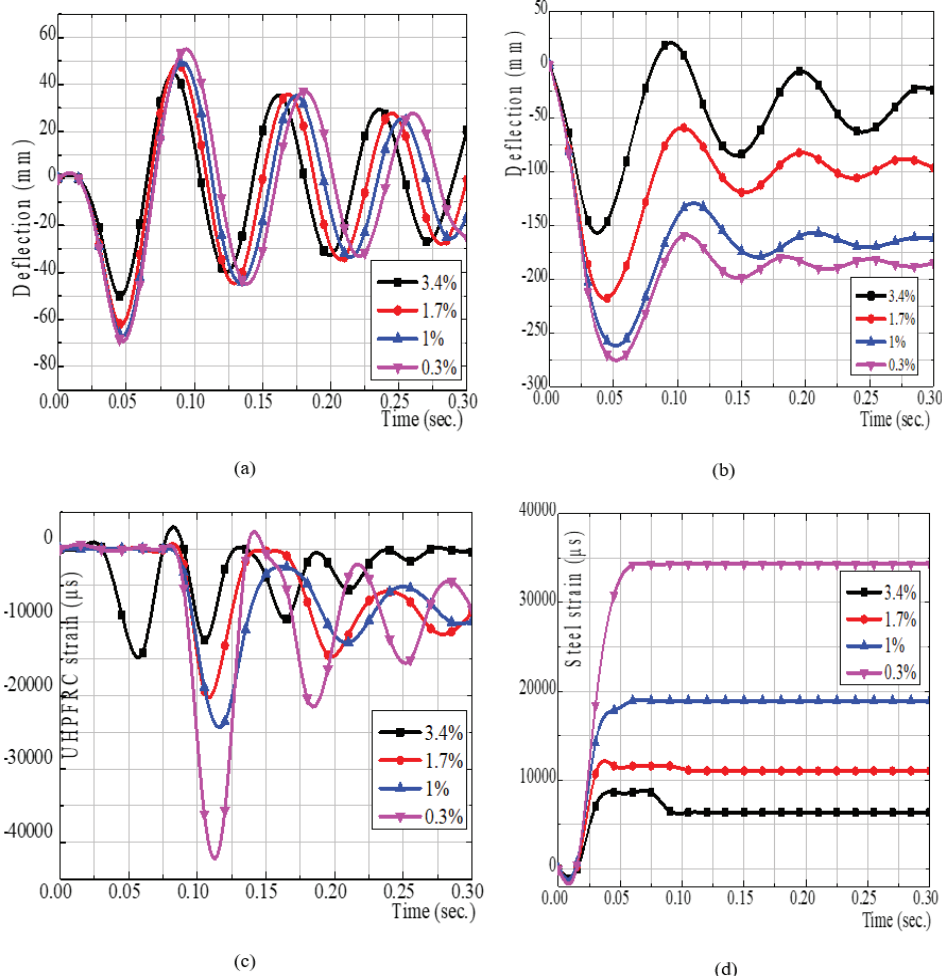


Figure 6. Maximum mid-span deflection of the panel in 19 m stand-off distance (a) and 9 m of stand-off distance (b); Strain of UHPFRC element (c) and strain of steel bar (d) in 9 m stand-off distance.

5. CONCLUSIONS

This research presented the results of the UHPFRC panel subjected to severe blast loading. The UHPFRC material was modeled using the Johnson-Holmquist 2 damage model, based on the platform of ABAQUS software and combined with the subroutine. The validity of the proposed model was verified against experimental results. The variations in deflection, UHPFRC strain, and damage of the UHPFRC panel, as well as the steel reinforcement strain, were also analyzed. A total of 16 models were calculated to evaluate the effect of panel thickness, stand-off distance, and steel reinforcement ratio on the structural behaviour of the UHPFRC panel under severe blast loading. From the results addressed in this research, the following conclusions are drawn:

- Johnson-Holmquist 2 damage model can be successfully utilized to simulate the process of the UHPFRC panel under blast loading.
- The subroutine established by the authors demonstrates the accuracy to analyze the UHPFRC panel under blast loading. Next phase, this subroutine can be developed for more complex structures such as the UHPFRC frame or tunnel under blast loading.
- Using UHPFRC panel with higher thickness reduced the maximum mid-span deflection and strain of the UHPFRC panel. As panel thickness decreases, damage mode of flexural failure is prone to transform into damage mode including flexural failure and shear failure. Increasing the UHPFRC panel thickness is one of the most efficient methods to improve the load capacity of this structure under blast loading. In the far-field regime, increasing the reinforcement ratio does not have a significant effect on the maximum mid-span deflection and damage state of the UHPFRC panel. However, in the near field regime, the blast loading resistance capacity of UHPFRC panels can be improved significantly by increasing the steel reinforcement bar ratio.
- Through numerical simulation, the design of protective structures such as panel using UHPFRC material to against blast load, is feasible. However, to definitely avoid the deformation and serious damage of the structure, the parameters such as thickness of panel, steel reinforcement bar ratio or blast loading scenario, are important and should be prudently considered.

REFERENCES

1. Li, J; Wu, C; Hao, H & Su, Y. Investigation of ultra-high performance concrete under static and blast loads. *Int. J. Prot. Struct.*, 2015, **6**(2), 217-234. doi: 10.1260/2041-4196.6.2.217
2. Tayeh, BA; Aadi, AS; Hilal, NN; Bakar, BHA; Al-Tayeb, MM & Mansour, WN. Properties of ultra-high-performance fibre-reinforced concrete (UHPFRC) - A review paper. *In AIP Conference Proceedings*, 2019, 2157(September). doi: 10.1063/1.5126575
3. Khairunnisa, M.; Zahid, M.Z.A.M.; Rafiza, A.R. Nurfitriah, I.; Zainol, N. Z.; Manaf, M. B. H. A.; Ahmad, M. M.; Aishah, S. N. M. N.; Noh, N. N.; Johari, M. Z. & Zaidi, A.S.S.M. Ultra high performance fibre reinforced concrete mixture proportion - A review. *In AIP Conference Proceedings*, 2018, 2030 (November). doi: 10.1063/1.5066938
4. Wu, Z.; Shi, C.; He, W. & Wang, D. Static and dynamic compressive properties of ultra-high performance concrete (UHPC) with hybrid steel fibre reinforcements. *Cem. Concr. Compos.*, 2017, **79**, 148-157. doi: 10.1016/j.cemconcomp.2017.02.010
5. Yoo, D.Y. & Banthia, N. Mechanical properties of UHPFRC: A review. *Cem. Concr. Compos.*, 2016, **73**, 267-280. doi: 10.1016/j.cemconcomp.2016.08.001
6. Buttignol, T.E.T.; Sousa, J.L.A.O. & Bittencourt. Ultra High-Performance Fibre-Reinforced Concrete (UHPFRC): a review of material properties and design procedures. *In Revista IBRACON de Estruturas e Materiais*, 2017, **10**(4), 957-971. doi: 10.1590/s1983-41952017000400011
7. Azmee, N.M. & Shafiq, N. Ultra-high performance concrete: From fundamental to applications. *Case Stud. Constr. Mater.*, 2018, **9**. doi: 10.1016/j.cscm.2018.e00197
8. Anandavalli, N.; Lakshmanan, N.; Iyer, N.R. & Prakash, A. Behaviour of a Blast Loaded Laced Reinforced Concrete Structure. *Def. Sci. J.*, 2012, **62**(5), 284-289. doi: 10.14429/dsj.62.820.
9. Duan, Z-P; Zhang, H-Y & Wu, H-J. Rear-surface collapse of finite thickness concrete targets under internal explosion. *Def. Sci. J.*, 2012, **62**(5), 295-299. doi: 10.14429/dsj.62.1237
10. Ngo, T; Mendis, P; Gupta, A & Ramsay, J. Blast loading and blast effects on structures - An overview. *Electron. J. Struct. Eng.*, 2007, **7**(September 2016), 76-91
11. Shukla, P; Desai, A & Modhera, C. Study of dynamic response of wall panel subjected to blast load. 2018, **1**, 51-44. doi: 10.29007/lcct
12. Ellis, B.D; Dipaolo, BP; McDowell, DL & Zhou, M. Experimental investigation and multiscale modeling of ultra-high- performance concrete panels subject to blast loading. *Int. J. Impact Eng.*, 2014, **69**, 95-103. doi: 10.1016/j.ijimpeng.2013.12.011
13. Giovino, G; Olmati, P; Garbati, S & Bontempi, F. Blast resistance assessment of concrete wall panels: Experimental and numerical investigations. *Int. J. Prot. Struct.*, 2014, **5**(3), 349-366. doi: 10.1260/2041-4196.5.3.349
14. Lin, X.; Zhang, Y.X. & Hazell, P.J. Modeling of steel-reinforced concrete panels under blast loads. *Appl. Mech. Mater.*, 2014, **553**, 100-108. doi: 10.4028/www.scientific.net/AMM.553.100
15. Iannitti, G.; Bonora, N.; Curiale, G. Murob, S.D.; Marfaia, S.; Ruggieroa, A.; Saccoc, E.; Scafati, S. & Testaa, G. Analysis of reinforced concrete slabs under blast loading. *In Procedia Structural Integrity*, 2018, **9**, 272-278. doi: 10.1016/j.prostr.2018.06.035
16. Oswald, C.J. & Bazan, M. Performance and blast

- design for non-load bearing precast concrete panels. *In Proceedings of the 2014 Structures Congress*, 2014, 143-154.
doi: 10.1061/9780784413357.014
17. Burrell, R. Performance of steel fibre reinforced concrete columns under shock tube induced shock wave loading. 2012, (August), 248
 18. Xu, J.; Wu, C.; Xiang, H.Su, Yu; Li, Zhong-Xian; Fang, Qin; Hao, Hong; Liu, Zhongxian; Zhang, Yadong & Li, Jun Behaviour of ultra high performance fibre reinforced concrete columns subjected to blast loading. *Eng. Struct.*, 2016, 118, 97-107.
doi: 10.1016/j.engstruct.2016.03.048
 19. Rizwanullah, R. & Sharma, H.K. Influence of critical parameters on UHPFRC structural elements subjected to blast loading. *SN Applied Sciences*, 2020, (September 2019).
doi: 10.1007/s42452-020-2259-5
 20. Mao, L.; Barnett, S.; Begg, D.; Schleyer, G. & Wight, G. Numerical simulation of ultra high performance fibre reinforced concrete panel subjected to blast loading. *Int. J. Impact Eng.*, 2014, 64, 91-100.
doi: 10.1016/j.ijimpeng.2013.10.003
 21. Brian, C. & Rebstrost, M. Ductal – A High-Performance Material for Resistance to Blasts and Impacts. *Aust. J. Struct. Eng.*, 2006, 7(1), 37-45.
doi: 10.1080/13287982.2006.11464962
 22. Holmquist, T.J.; Johnson, G.R. & Cook, W.H. A Computational constitutive model for concrete subjected to large strains, high strain rates and high pressures. *In 14th International symposium, Warhead mechanisms, terminal ballistics; Quebec; Canada, 1993, Vol 2, 591–600*
 23. Johnson, G.R. & Holmquist, T.J. A computational constitutive model for brittle materials subjected to large strains, high strain rates and high pressures. *Shock Wave and HighStrain Rate Phenomena in Materials. In CRC Press: Boca Raton, FL, USA, 1992, (1), 1075–1081.*
 24. Lee, K; Kim, T & Kim, J. Local response of W-shaped steel columns under blast loading. *Struct. Eng. Mech.*, 2009, 31(1), 25-38.
doi: 10.12989/sem.2009.31.1.025
 25. Corp, DSS. Simulia. ABAQUS 6.14 User’s Manuals. Springer Netherlands; 2016,
doi: 10.1007/s40069-016-0157-4
 26. Luccioni, B; Ambrosini, D & Danesi, R. Blast load assessment using hydrocodes. *Eng. Struct.*, 2006, 28(12), 1736-1744.
doi: 10.1016/j.engstruct.2006.02.016
 27. Yu, R.; Spiesz, P. & Brouwers, H.J.H. Numerical Simulation of Ultra-High Performance Fibre Reinforced Concrete (UHPFRC) Under High Velocity Impact of Deformable Projectile. *In Distribution A: For Public Release*, 2013, 1-10
 28. David W Hyde. User’s Guide for Microcomputer Programs ConWep and FunPro, Applications of TM 5-855-1, Fundamentals of Protective Design for Conventional Weapons. Vicksburg, Miss. : U.S. Army Engineer Waterways Experiment Station, 1988.
 29. Prueter, PE. Using explicit finite element analysis to simulate blast loading on hazardous chemical storage tanks. 1-15.
 30. Hallquist, JO; Wainscott, B & Schweizerhof, K. Improved simulation of thin-sheet metalforming using LS-DyNA3D on parallel computers. *J. Mater. Process. Tech.*, 1995, 50(1-4), 144-157.
doi: 10.1016/0924-0136(94)01376-C
 31. MA, S. Mechanical effects of air shock waves from explosions according to experiments. *In Physics of explosion, USSR Academy of Sciens, Moscow, 1953, 1, 77-110*
 32. Krauthammer, T. Blast effects and related threats. Technical paper, Protective Technology Centre, Penn State University, 1999.
 33. M. Smith, S.; McCann, D & K. Blast resistant design guide for reinforced concrete structures. *In Portland Cement Association, 2009.*

CONTRIBUTORS

Mr Viet-Chinh Mai is pursuing a PhD at Kumoh National Institute of Technology, South Korea. His research interests are ultra high performance concrete, steel, and composite structure.

In the current study, he conceived of the presented ideas, developed the theory, and performed the computations.

Dr Ngoc-Quang Vu is working as a Professor of Structural Engineering at Le Quy Don Technical University, Ha Noi, Viet Nam.

In this study, he encouraged all authors to investigate specific aspects and supervised the findings of this work.

Dr Van-Tu Nguyen is working as a senior lecturer and researcher in Dept. of Civil Engineering, Le Quy Don Technical University.

In this study, he contributed to the interpretation of the results, provided critical feedback, and helped shape the research, analysis, and manuscript.

Mr Hoang Pham is presently working as a senior lecturer and researcher in Dept. of Civil Engineering, Le Quy Don Technical University.

In the current study, he carried out the calculations and wrote the manuscript.